Acta Technologica Agriculturae 4
Nitra, Slovaca Universitas Agriculturae Nitriae, 2025, pp. 204–211

IMPROVING ENERGY MANAGEMENT OF HYBRID POWER SUPPLY SYSTEM FOR LIVESTOCK FARM WITH RENEWABLE ENERGY SOURCES AND ELECTRIC TRANSPORT

Olexandr SHAVOLKIN[1], Iryna SHVEDCHYKOVA[1], Yurii HAMAN[1], Ladislav TÓTH*[2]

[1]Kyiv National University of Technologies and Design, Faculty of Engineering and Information Technologies, Department of Computer Engineering and Electromechanics, Kyiv, Ukraine, shavolkin.oo@knutd.edu.ua (O.S.), shvedchykova.io@knutd.edu.ua (I.S.), yurii.hamann@gmail.com (Y.H.)

[2]Slovak University of Agriculture in Nitra, Faculty of Engineering, Institute of Electrical Engineering, Automation, Informatics and Physics, Nitra, Slovakia

*correspondence: ladislav.toth1@uniag.sk

The paper focuses on farm energy consumption reduction by using control according to the forecast, considering possible deviations in generation and load from the calculated ones. The correction of the power consumption value is applied according to the deviation of the main battery state of charge from the calculated schedule, with the start value set based on the forecast. For grid mode, it is proposed to use a monotonous decrease of the battery's state of charge during the day, reducing energy losses. This is also facilitated by levelling the load schedule by electric transport battery charging. An algorithm for calculating power consumption has been developed to create a schedule for the battery state of charge, taking into account peak consumption and depth of discharge limitations. This, together with the exclusion of correction at certain time intervals, ensures the maximum use of the battery's energy capacity for renewable energy consumption. Simulation under different load schedules confirms the possibility of decreasing consumption by 3–5% due to the proposed changes in the charge schedules of electric transport and the state of charge of the main storage battery of the system, at a depth of discharge of no more than 52%.

Keywords: hybrid system with renewable energy sources; gas generator; electric transport; forecast of generation; power correction; schedule of the battery state of charge

Recently, there has been a trend toward using hybrid power supply systems with multiple renewable energy sources (RES) for small-scale objects, particularly those in the agro-industrial sector (Zeeshan and Aized, 2023). Such systems typically contain a photovoltaic system (PVS), wind turbines (WG), and a storage battery (SB), and can be connected to the grid. This arrangement aims to reduce electricity consumption from the grid and increase power supply reliability. The use of electric transport (ET) not only decreases the release of greenhouse gases (Khodkam et al., 2025), but its SBs can be utilised to control the object's energy consumption. When the mains voltage is off and RES energy is insufficient, diesel generators (DG) or other generators are employed.

The prospects for using hybrid renewable systems (HRES) in various areas are now beyond doubt. The issues of HRES are subject to consideration by many researchers; specifically, methods of energy management for HRES with PV, WG, and SB are presented in review papers (Olatomiwa et al., 2016; Meng et al., 2016; Faccio et al., 2018; Lamnatou et al., 2024).

The feasibility of combining PVS, WG, DG, and SB into HRES for a residential building is considered in Thirumalai et al. (2024). The work by Ganthia et al. (2024) presents an energy management system using HRES with PVS, WG, and SB for a small enterprise. Many papers are devoted to optimising the parameter selection of grid-tied HRES (Kumar et al., 2022) and for standalone use (Fakhfour and Pourfayaz, 2024; Bourek et al., 2025). Monitoring energy consumption and accessing acquired data in real time is also necessary, which can be provided by an online connection using an LTE wireless communication network (Vacho et al., 2022).

Modern SBs, particularly the LiFePO4 type, have high charge/discharge currents and significant resources. However, use at a depth of discharge (*DoD*) of 80% provides 3000 discharge cycles, while at *DoD* = 50%, the number of cycles is 5000. In Muala et al. (2024), along with energy cost minimisation, the extension of SB life is considered. It is noted that the *DoD* is important in the operation of SB and significantly affects its life cycle. The work by Rekioua et al. (2023) notes that HRES control must maintain the SB's state of charge (*SoC*) at a level that prevents power outages and extends the SB's life.

Alanazi et al. (2024) argue that to ensure electricity supply at the lowest possible cost while optimally responding to load requirements, the control system must perform real-time energy forecasts for RES, control energy storage components, and regulate loads. In Gunmi et al. (2024), the energy management system is based on the *SoC* = (100 – *DoD*)% of the SB, supercapacitor, and hydrogen tank, as well as the forecast of solar radiation, wind speed, and load for the day ahead.

Increasing the reliability of the RES generation W_{RF} forecast using neural networks is presented by Díaz-Bello et al. (2024). A genetic algorithm based on a wavelet neural network is used by Zhang and Zhang (2022) to optimise the prediction of PV generation.

The issue of controlling a HRES with PV, WG, and SB using the forecast of RES generation and control of power P_g consumed from the grid is considered by Shavolkin et al. (2022). At the same time, the *SoC*(t) schedule is formed according to the calculated load power schedule $P_L(t)$ and the forecast of RES generation $P_{RF}(t)$. It also excludes energy consumption from the grid W_g during peak demand hours. The system's autonomous operation mode (AOM) is not considered for grid disconnection.

Shavolkin and Haman (2024) consider using HRES with PVS, WG, and SB for a small livestock farm in an AOM when the mains voltage is turned off using an electric gas generator (EGG). At the same time, the farm uses its plant for biogas production. To maintain the loading of EGGs within acceptable limits, the power of the main SB0 P_{B0} is regulated according to the $P_{RF}(t)$.

However, the possible error of the forecast can be up to 15–20% (Abdelsattar et al., 2024; Iyengar et al., 2017). An underestimated P_{RF} leads to a decrease in the degree of RES use. At the same time, an overestimated forecast leads to an increase in the *DoD*. This also applies to deviations of the P_L load relative to the calculated (planned) one.

The possibility of adjusting the SB power P_B is declared in Shavolkin and Haman (2024), which compensates for the deviation of P_R relative P_{RF} and the P_L relative to the calculated one while maintaining the value of the EGG power P_{EG} within the established limits. The implementation of this is not reflected in the results. The consideration is limited to ensuring the functioning in AOM.

Another approach with the correction of the power value P_g by the deviation of the *SoC* relative to the given schedule *SoC*(t), calculated by $P_{RF}(t)$, is proposed by Shavolkin et al. (2023a). The effectiveness of correction for forecast errors of up to 10% is shown. The possibility of working at a higher forecast error value must be assessed. A regulation system with three control channels is used: grid current, PV current, and SB current. For practical implementation, using the standard functions of hybrid inverters is desirable.

Thus, several issues regarding HRES control, both in the AOM and grid-tied operation, have not been sufficiently studied. This applies to controlling energy consumption with an increase in the degree of RES energy use, limiting peak value P_g and reducing the *DoD* of the SB, taking into account the possible W_R deviation from W_{RF}, which requires additional study.

The purpose of the work is to improve the control of HRES according to the RES generation forecast for a decrease in energy consumption from the grid, limitation of peak consumption from the grid and the *DoD*, taking into account the possible deviation of RES generation relative to the forecast and load relative to the calculated one.

Material and Methods

Classical methods for calculating and analysing energy processes in electrical circuits at the active power level are used in the research. Since the analysis is performed for the daily cycle, transients are not taken into account. Energy losses in energy converters and storage batteries are accounted for through efficiency.

Accounting for the energy use of ET batteries is simplified using the recommended discharge and charge schedules in time. To implement energy control, the standard modes of serial hybrid inverters of the SUN-30K Deye type (China) are considered.

The control is carried out according to the RES forecast and the estimated (planned) farm consumption. A controlled parameter is the *SoC* calculated schedule of the main SB of the PVS, which determines the limitation of the *DoD* value. The limit of peak consumption from the grid is set by the calculated graph of the power $P_{gR}(t)$, consumed from the grid. To minimise the impact of deviations in RES generation and load relative to the calculated values, a closed-loop by deviation *SoC* control system is used. Compensation for the deviation of the current *SoC* value from the taken value is carried out by correcting the P_{gR} value. The corresponding value of the correction power P_K is proportional to the *SoC* deviation. Since the rate of *SoC* change is low, control with a discreteness of 0.25 hours is considered. When the RES energy is excessive, the PV generation control is carried out at $P_K = 0$. When calculating the *SoC* graph, the charging characteristic of the SB specified by the manufacturer is used, taking into account the charge zone at constant voltage, which helps improve the accuracy of correction.

The formation of *SoC*(t) allows for reducing energy losses at a schedule with a monotonic SB discharge while limiting the use of additional charge/discharge cycles. At the same time, an increase in the degree of RES consumption is possible due to the correction of the *SoC* value to maximise the use of the energy power of the main SB with a regulated charge of the SB of ET during the hours of maximum P_{PV}.

A gas generator with a restriction of limit and minimum power is used in AOM, which excludes its overload and contributes to the economical use of biogas.

The mathematical model uses analytic expressions for steady-state regimes that correspond to generally accepted calculation methods. The charging and discharge characteristics of the LiFePO4-type battery, according to the manufacturer's data, are considered when describing the SB models. The RES generation was set according to archival data for Kyiv. At the same time, the possible deviation of RES generation relative to the forecast data (±20%) and load consumption relative to the calculated schedule was taken into account. The proposed solutions are considered for a specific application but with different load schedules and the same daily consumption, making it possible to generalise the results obtained to a certain extent.

Results and Discussion

Substantiation and implementation of the HRES control mechanism; energy consumption, HRES structure, and general description of the operation

This work is a continuation of the research by Shavolkin and Haman (2024), where the HRES for a small livestock farm without exporting energy to the grid was considered. The HRES contains a PV module with a hybrid grid inverter and a main battery SB0, a WG module with grid inverter, gas generator EGG, and a charger with two-way conductivity (V2G) for ET with SB1 and SB2. Consideration is limited by the November-April period when cattle are on the farm. The load graph in the AOM is saved (curve 1 in Fig. 1). When working with the grid, the load relative to the AOM increases (curve 2 in Fig. 1). The variant of equalizing the load by time while maintaining consumption is also considered (AOM – curve 3, work with the grid – curve 4). Subsequently, 1 and 2 are designated as variant V1, and 3 and 4 are designated as variant V2.

By working with the grid, we take a fixed operation schedule (charge) for ET. Operation is from 6:00 to 17:00. During peak hours, charging is not carried out. In the grid-on mode, the reference value of the charge energy $W_{B1,2}$ of the SB1, 2 is constant (10 kWh is accepted), and for the AOM, it is calculated according to the forecast.

Power balance in the system:

$$P_g + P_R \cdot \eta_C - P_{B0} - P_{LC} = 0 \quad (1)$$

where: $P_R = (P_{PV} + P_W)$; P_{PV} – *PV* power; P_W – *WG* power; P_{B1} and P_{B2} – powers of SB1 and SB2; $P_{LC} = (P_L + P_{B1} + P_{B2})$; η_C – efficiency of RES converter and invertor; P_{B0} – power of SB0

The value P_{B0} at the SB0 charge (*SoC*) $Q^* \geq Q^*_d (Q^* = 100 \cdot Q/Q_R$; Q_R – *SoC*, which corresponds to SB0 capacitance C_B (Ah), Q^*_d – corresponds to the start of charge with a U_{BC} = *const*) is limited by the SB0 charge characteristic $P_B(Q^*)$. With a common charger, the charge of SB1 and SB2 is carried out alternately according to the reference value $P_{B1,2}$. At the interval (t_0, t_1) according to the specified $P_g(P_{EG})$, measured values P_R, P_L, reference P_{B0} ($P_{B0} \leq P_B(Q^*)$ and $P_{B0} \leq P_{BMAX}$) is determined by reference $P_{B1,2}$.

Formation of the state of charge of the main storage battery

For the taken graph $P_L(t)$ at the initial value Q^*_1 and value Q^*_6 at the beginning of the evening peak, we have a fixed degree of discharge SB0 ($\Delta Q^*_{16} = c = (\Delta Q^*_{12} + \Delta Q^*_{45}) - (\Delta Q^*_{24} + \Delta Q^*_{56}) = a - b$, where ΔQ^*_{24}, ΔQ^*_{56} – charge increments; ΔQ^*_{12}, ΔQ^*_{45} – discharge decrements).

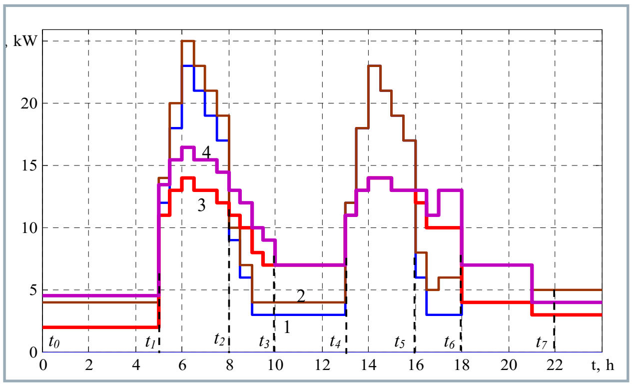

Fig. 1 Graphs of the load for livestock farm

With this, the loss of energy in SB0:

$$\Delta W = 0.01 W_{B0}\left[c(1-\eta_C \cdot \eta_B) + b\left(\frac{1}{\eta_C \cdot \eta_B} - \eta_C \cdot \eta_B\right)\right] \quad (2)$$

where: η_B – the efficiency of SB0; $W_{B0} = U_B \cdot C_B$ – SB0 energy capacitance

At c = *const*, the value b is variable. In the case of W_{B0} = 80 kWh and b reduction of 10%, ΔW = 1.68 kWh. Reducing $\Delta Q^* > 0$ is achieved by increasing Q^*_2, decreasing Q^*_4, or increasing Q^*_2 and decreasing Q^*_4 simultaneously. Thus, forming $Q^*_R(t)$ with a monotonous reduction Q^* in time is advisable. This is not possible in AOM with the accepted power limit P_{EG}.

The schedule $Q^*_R(t)$ must be different according to the value W_R. The boundary value W_{RB} can be determined according to ΔQ^*_{34} at the interval (t_3, t_4) at $P_{g34} = 0$:

$$\Delta Q^*_{34} = \frac{W_{RF34} \cdot \eta_C - W_{L34} - W_{B12.34}}{0.01 W_{B0}} \eta_B \cdot \eta_C \quad (3)$$

where: W_L – load energy; $W_{B12.34}$ – the energy of SB1, 2

When $\Delta Q^*_{34} > 0$, there is a "high" level, when the choice of values Q^*_1 and Q^*_2, and the value of P_{gR}, is also carried out for the accepted restrictions. If $\Delta Q^*_{34} \leq 0$, the schedule $Q^*_R(t)$ is set with a monotonous decrease in value Q^* in time, which may be unchanged.

Discrete in-time correction of the value P_g by deviation Q^* relatively $Q^*_R(t)$ at the interval (t_1, t_0) is considered.

The value of $Q^*_R(t)$:

$$Q^*_R = Q^*_{1M} + B\int_{t1}^{t0} P_{B0}\,dt = Q^*_{1M} + B\int_{t1}^{t0}(P_{RF} \cdot \eta_C + P_{gR} - P_{LC} - P_{B12})\,dt \quad (4)$$

where: $B = \frac{\eta_C \cdot \eta_B}{0.01 W_B}$ – at SB0 charge;

$B = \frac{1}{0.01 W_B \cdot \eta_C \cdot \eta_B}$ – at SB0 discharge

For RES generation, less than the boundary value $W_R \leq W_{RB}$, schedule $Q^*_R(t)$ is set by linear dependencies on intervals (t_1, t_6), (t_6, t_7), (t_7, t_0) with a restriction of the *DoD* ≤30%.

Value P_{B0} in constant voltage charge mode U_{BC} at $Q^* \geq Q^*_d$ is $P_{B0} = U_{BC} \cdot C_B \cdot I^*_B(Q^*)$, where $I^*_B(Q^*)$ – the charging characteristic in relative units.

The value of the power consumed from the grid P_g (or P_{EG}):

$$P_g = P_{gR} + P_K \frac{k}{T_f \cdot p + 1} \quad (5)$$

where: $P_K = \Delta q_i \cdot K$ – correction power; $\Delta q_i = (Q^*_{Ri} - Q^*_{Mi})$; K – regulator transmission coefficient; T_f – the constant of time of filter; k – variable that determines the area of correction action. There is a variable $k = 0$ at intervals with P_{PV} regulation to zero energy exports to the grid (or *EGG*)

In the AOM value, P_{EG} is determined with the restriction $P_{EGMIN} \leq P_{EG} \leq P_{EGMAX}$.

The value of the coefficient of transmission of the power regulator:

$$K = \frac{0.01 \cdot W_{B0} \cdot \eta_C \cdot \eta_B}{\Delta t} \quad (6)$$

The power that the RES can provide in the maximum power point tracking mode (MPPT) for AOM is $P_{RM} = P_{EG} + P_{RESM} \cdot \eta_C$. The power that can be consumed is $P^1_R = P_{LC} + P_{B0}$. The power of energy sources, taking into account the P_{PV} regulation:

$$P_R = \begin{cases} P^1{}_R, \text{ if } P_{RM} > P^1{}_R \\ P_{RM}, \text{ if } P_{RM} \leq P^1{}_R \end{cases} \quad (7)$$

The actual value of power consumed from the EGG (or grid):

$$P_{EG} = \begin{cases} (P_R - P_{RESM} \cdot \eta_C), \text{ if } P_R > P_{RESM} \cdot \eta_C \\ 0, \text{ if } P_R < P_{RESM} \cdot \eta_C \end{cases} \quad (8)$$

Value $k = 1$ if $\left(P_{RESM} \cdot \eta_C - (P_R - P_{EG}) - P_{g1}\right) < 0$ (P_{g1} is the minimum value).

Grid-tied mode

The value of $W_{B\,12.24}$ is set fixed. If $W_R > W_{RB}$ and $Q^*_2 < 40\%$, the maximum value of $P_{B\,12.24}$ is set for both ET. In other cases, the power of one of the ETs $P_{B\,1.24}$ decreases, and the charge time increases. Value P_{gR} at peak tariff intervals is taken $P_{gR23} = P_{gR67} = 0$, $P_{B\,12.23} = P_{B\,12.67} = 0$. The schedule of ET1 and ET2 use (SB1, 2) is planned, taking into account the operating time with average energy consumption. The option of a tractor use from 6:00 was considered (removal of manure to a biogas generator plant, delivery of feed, etc.). After that, at 8:30 it connects to the charger, and a truck is used, which is charging from 11:30 to 13:00. The charging of SB1, 2 is also provided before the start and at the end of the evening peak tariff.

$W_R > W_{RB}$. Value ΔQ^*_{67} for the evening peak at interval (t_6, t_7) at $P_{gR67} = 0$ is:

$$\Delta Q^*_{67} = \frac{W_{R67} \cdot \eta_C - W_{L67}}{0.01 W_{B0} \cdot \eta_B \cdot \eta_C} \quad (9)$$

Values $Q^*_7 \geq 55\%$, $Q^*_6 = (Q^*_7 + \Delta Q^*_{67})$. At $Q^*_7 = 55\%$, $Q^*_0 = 90\%$, the charge increments over the interval (t_7, t_0) and the corresponding value W_{g70} is determined. For $P_{gR24} = 0$:

$$\Delta Q^*_{24} = \frac{W_{R24} \cdot \eta_C + W_{gR24} - W_{L24} - W_{B12.24}}{0.01 WB_0} \eta_B \cdot \eta_C \quad (10)$$

$$\Delta Q^*_{12} = \frac{W_{R12} \cdot \eta_C + W_{gR12} - W_{L12}}{0.01 W_{B0} \cdot \eta_B \cdot \eta_C} \quad (11)$$

Value $Q^*_2 = (Q^*_4 - \Delta Q^*_{24})$ at $Q^*_4 \rightarrow 100\%$ is limited to $Q^*_2 \geq 30\%$. At $P_{gR12} = 0$ by (11), ΔQ^*_{12} and $Q^*_1 = (Q^*_2 - \Delta Q^*_{12})$ are determined. In the case of $Q^*_1 \leq 100\%$, we have a limit $Q^*_1 \geq 80\%$ with a corresponding change of Q^*_2 in case of using restriction $Q^*_1 = 80\%$. If $Q^*_1 > 100\%$, $Q^*_1 = 100\%$ is accepted by determining the appropriate values ΔQ^*_{12} and P_{gR12}. Value Q^*_5 is accepted as $Q^*_5 > Q^*_6$. Under ΔQ^*_{45}, ΔQ^*_{56}, $P_{gR45} = P_{gR56}$ are determined.

Autonomous operation mode

The P_{EGR} restrictions are introduced as $P_{EGRMAX} \leq 0.9\ P_{EGRate}$. This provides the possibility to increase P_{EG} in case of $W_R < W_{RF}$ and P_L is above the calculated. At $\Delta Q^*_{24} \geq 0$, the task of providing the maximum possible charge of SB1, 2 at the interval (t_2, t_4) is solved, and recommendations for charging the SB1, 2 in the evening hours are also determined. Let's limit the minimum value $Q^*_2 \geq 30\%$. The maximum value $Q^*_{2MAX} = (Q^*_1 - \Delta Q^*_{12MIN})$ is limited under the condition of $P_{EG12} = P_{EGRMAX}$. The value of P_{EG24} is determined, which corresponds to $\Delta Q^*_{24} = (Q^*_4 - Q^*_{2MAX})$ and $W_{B12.24} = W_{B12.24MAX}$:

$$P_{EG24} = \frac{W_{L24} + W_{B12.24} + \dfrac{0.01 \Delta Q^*_{24} \cdot W_{B0}}{\eta_C \cdot \eta_B} - W_{R24} \cdot \eta_C}{(t_4 - t_2)} \quad (12)$$

If $P_{EG24} < 0$, then $P_{EG24} = 0$, and ΔQ^*_{24} is determined as:

$$\Delta Q^*_{24} = \frac{W_{R24} \cdot \eta_C - W_{L24} - W_{B12.24}}{0.01 W_{B0}} \eta_B \cdot \eta_C \quad (13)$$

For this $Q^*_2 = (Q^*_4 - \Delta Q^*_{24})$, $\Delta Q^*_{12} = (Q^*_1 - Q^*_2)$ and, if $Q^*_2 \geq 30\%$, value P_{EG12}:

$$P_{EG12} = \frac{W_{L23} - 0.01 \Delta Q^*_{12} \cdot W_{B0} \cdot \eta_C \cdot \eta_B - W_{R12} \cdot \eta_C}{(t_2 - t_1)} \quad (14)$$

If $Q^*_2 < 30\%$, then $Q^*_2 = 30\%$ is accepted, and the value P_{EG12} is corrected.

If, according to Eq. (12), there is $P_{EGMAX} \geq P_{EG24} \geq 0$, then $Q^*_2 = Q^*_{2MAX}$, $P_{EG12} = P_{EGMAX}$ are accepted. In case of $P_{EG24} > P_{EGMAX}$, then $P_{EG24} = P_{EGMAX}$, $Q^*2 = Q^*_{2MAX}$ is accepted, and the value $W_{B12.24}$ decreases:

$$W_{B1224} = W_{R24} \cdot \eta_C + W_{EG24MAX} - W_{L24} - \frac{\Delta Q^*_{24}\ 0.01 W_{B0}}{\eta_B \cdot \eta_C} \quad (15)$$

If $\Delta Q^*_{24} < 0$, P_{EG} is determined according to the value Q^*_2 at $W_R = 0$. In this case, the value $Q^*_2 \geq 76\%$. At this power value, given by the SB1, 2 at the interval (t_1, t_2):

$$W_{B12.12} = W_{L12} - W_{R12} \cdot \eta C - P_{EGMAX}\,(t_2 - t_1) - 0.01 \Delta Q^*_{12} \cdot W_{B0} \cdot \eta_B \cdot \eta_C \quad (16)$$

Under condition $Q^*_0 \rightarrow 90\%$, the values Q^*_6 and Q^*_5 at P_{EG60} and P_{EG56} are determined to be less than the maximum. $\Delta Q^*_{45} = (Q^*_4 - Q^*_5)$ is also determined. The energy value, given by the SB1, 2, is:

$$W_{B12.45} = W_{L34} - W_{RESF34} \cdot \eta_C - P_{EGMAX}\,(t_4 - t_3) - 0.01\ \Delta Q^*_{34} \cdot W_{B0} \cdot \eta_B \cdot \eta_C \quad (17)$$

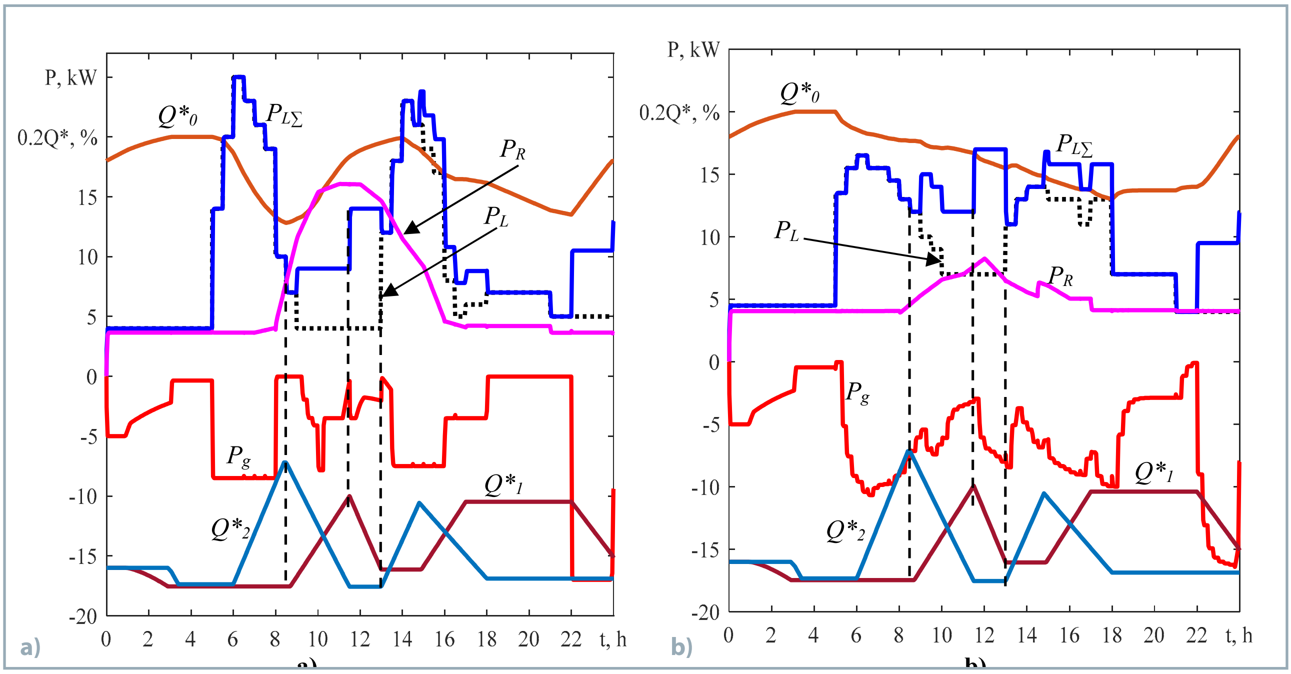

Fig. 2 Process plots in the daily cycle
a) $W_R > W_{RB}$; b) $W_R < W_{RB}$

If $W_{B12.45} < 0$, then $W_{B12.45} = 0$ is accepted, and the corresponding energy can be used to charge a more discharged one from the batteries SB1, 2.

Simulation results

The simulation of energy processes in the system was carried out using MATLAB/Simulink software based on the models from Shavolkin et al. (2023b) and Shavolkin and Haman (2024), at $P_{PV} = 30$ kW, $P_W = 5$ kW, $P_{EGG} = 7$ kW, $W_{B0} = 80$ kWh, $W_{B1} = 50$ kWh, $W_{B2} = 30$ kWh, $\eta_C = 0.94$, $\eta_B = 0.96$, $\Delta t = 0.25$ h.

In case $W_R = 0$, the maximum value P_{EG} using the discharge energy of SB1, 2 ($W_{B12.12} + W_{B12.34}$) = 32 kWh and the lack of a daytime charge of SB1, 2, we have $\Delta W = 1.18$ kWh at AOM. With the same energy consumption of EGG, the value Q^*_0 increased from 70.65% to 72.29%. The correction does not affect indicators.

Grid-tied mode at $W_R > W_{RB}$. For variant V1, the values of W_{RB1} in March and February are, accordingly, 133.5 kWh and 139.9 kWh. For V2 W_{RB2}, they are, accordingly, 151.2 kWh and 160.5 kWh.

In Table 1, indicators are shown at $Q^*_0 = 90\%$, $P_{B12.23} = 10$ kW, and at the duration of the day charge of SB1, 2 (1.5*2) = 3 hours ($W_{B12.23} = 30$ kWh); SB1, 2 charges at the interval (t_0, t_1) were not carried out (initial *SoC* is 80%). The values are $P^*_R = P_R/P_{RF} = 1$, $P^*_L = P_L/P_{LF} = 1$; correction limitations and, accordingly, energy consumption during peak hours was not carried out. The value W_{RF} corresponds to the maximum value, at which all RES energy, in case of reduction Q^*_2, is used for consumption. When $P^*_R = 0.85$ and $P^*_L = 1.15$ (marker *), there is a reduction of Q^*_2 to 26%. Increasing the *DoD* to 74% with one deep discharge is justifiable.

In Table 2, the indicators at $W_R > W_{RB}$ (for February) and $W_R \leq W_{RB}$ (for March and December), taking into account the charge of SB1, 2 are presented. The coefficients k_3, k_2, and k_1 determine the reduction of energy costs according to tariffs. The ratios are accepted: for 3 tariffs – night (preferential)/semi-peak (daytime)/peak 0.4/1/1.5; for 2 – night/day 0.4/1. The sign (+) – in the case of correction, sign (-) – without correction. The absence of a limit on

Table 1 Indicators in the case of operation with the grid with high RES generation

W_R (kWh)	Q^*_1 (%)	Q^*_2 (%)	Q^*_7 (%)	W_g (kWh)	$W_{RF\eta C}$ (kWh)	Q^*_1 (%)	Q^*_2 (%)	Q^*_7 (%)	W_g (kWh)
March V1					**March V2**				
218.3	100	37.3	75	65.12	227.9	100	56.5	79	57.62
218.3	92	30	75	56	227.9	80	37.5	77	52
218.3*	92	26	72	118.2	227.9*	80	35.5	76	117
February V1					**February V2**				
206.6	100	41	72	72.32	216.9	100	50	67	61.88
206.6	90	30.7	69	65.46	216.9	90	40	65	54.85
206.6*	90	29.3	68	126.6	216.9*	90	38	64	116.3

the peak consumption of P_P corresponds to (-), $P_P = 0$ or 1 kW corresponds to the limitation of peak power. When 10/10, the values are $P_{B1} = 10$ kW and $P_{B2} = 10$ kW by a duration of 1.5 hours. When 5/10, the value is $P_{B1} = 5$ kW by a duration of 3 hours, PB2 = 10 kW for 1.5 hours.

The process plots of $P_{L\Sigma} = (P_L + P_{B1} + P_{B2})$, P_L, P_R, P_g, Q^*_0, Q^*_1, Q^*_2 when $P^*_R = 1$, $P^*_L = 1$ are shown in Fig. 2 (process plots of P_g, Q^*_1, Q^*_2 are with a minus sign). The dotted line highlights the day charge zone of SB1, 2. Figure 3a corresponds to $W_R > W_{RB}$ (February $W^*_{RF} = 160.5$ kWh) for V1; Figure 3b corresponds to $W_R \leq W_{RB}$ for V2 (December $W^*_{RESF} = 116$ kWh).

The technological shutdown of the EGG after 8 hours by 0.5 hours is taken into account in the AOM. At $W_R = 0$ without a daytime charge of the SB1, 2, use for ET1 and ET2 is limited to 0.5 hours with a final value of the *DoD* ≥20%. The indicators for the AOM are shown in Table 3. They take into account the charge of SB1, 2 at the interval at (t_2, t_3) by W_R. It provides $\Delta Q^*_{24} > 0$ and a complete cycle of ET use. Also, in Table 3, there is an option with an SB 1,2 charge limitation in case of insufficient RES generation ($W_{RF} = 113.5$ kWh). With the same specific energy consumption, the ET use is reduced by a third. In the case of $W_R = 36.9$ kWh and without the charge of SB1, 2 in the daytime, it is possible to use ET

Table 2 Indicators in the case of operation with the grid for RES generation above and below the boundary generation

P^*_R (relative units)	P^*_L (relative units)	W_{RF} (kWh)	Variant	Correction	$P_{B12.23}$ (kWh)	P_P (kWh)	Q^*_1 (%)	Q^*_2 (%)	Q^*_7 (%)	k_3 (relative units)	k_2 (relative units)	k_1 (relative units)	W_g (kWh)
$W_R > W_{RB}$													
1	1	186.1	2	+	10/10	–	100	57	65	3.817	3.368	2.99	85.26
1	1	186.1	2	+	5/10	–	100	57	65	3.88	3.448	3.05	82.79
1	1	186.1	2	+	5/10	0	100	57	65	3.951	3.445	3.046	82.89
0.85	1.15	186.1	2	+	5/10	–	100	55	63.5	2.306	2.171	2.034	139.4
0.85	1.15	186.1	2	+	5/10	0	100	49	55	2.388	2.111	1.983	143.1
0.85	1.15	186.1	2	+	5/10	1	100	52	60	2.361	2.138	2.007	141.3
0.85	1.15	186.1	2	-	5/10	0	100	–	5	–	–	–	–
1	1	160.5	1	+	5/10	–	100	64	67	2.813	2.551	2.338	108.7
$W_R < W_{RB}$													
1	1	128.3	1*	+	10/10	–	100	60	67	2.07	1.887	1.782	143.2
1	1	128.3	1	+	10/10	–	100	90	70	2.01	1.942	1.824	139.8
1	1	128.3	1	+	5/10	–	100	88	70	2.061	1.972	1.846	136.5
1	1	128.3	1	+	5/10	0	100	86	57	2.169	1.951	1.827	138
1	1	128.3	1	+	5/10	1	100	87	68	2.135	1.97	1.944	136.7
0.85	1.15	128.3	1	+	5/10	–	100	85	69	1.644	1.604	1.538	186
0.85	1.15	128.3	1	+	5/10	0	100	80	48	1.757	1.584	1.503	190.3
0.85	1.15	128.3	1	+	5/10	1	100	82	55	1.72	1.582	1.515	188.8
0.85	1.15	128.3	1	-	5/10	–	100	–	$Q^*_3 = 0$	–	–	–	–
1	1	116	2	+	5/10	–	100	86	70	1.801	1.777	1.736	146

correction (+ yes, - no)

Table 3 Indicators in the autonomous operation mode

P^*_R (relative units)	P^*_L (relative units)	W_{RESF} (kWh)	Variant	$P_{B12.23}$ (kWh)	W_{B12} (kWh)	Q^*_1 (%)	Q^*_2 (%)	Q^*_4 (%)	Q^*_7 (%)	Q^*_0 (%)	W_{EG} (kWh)
1	1	128.3	1	10/10	0	100	62.5	55	78	90	105.4
1	1	128.3	1	5/10	0	100	62.5	56	79	90	103.5
0.9	1.1	128.3	1	5/10	0	100	58	43	71	85.44	127.1
1	1	128.3	2	10/10	0	100	83.5	70	77	90	103
1	1	128.3	2	5/10	0	100	83.3	66.5	76	90	100.3
1	1	113.5	1	2/4	0	100	62	57	75	90	100.9
1	1	36.9	2	0/0	-16	100	88	77	76	90	132.8

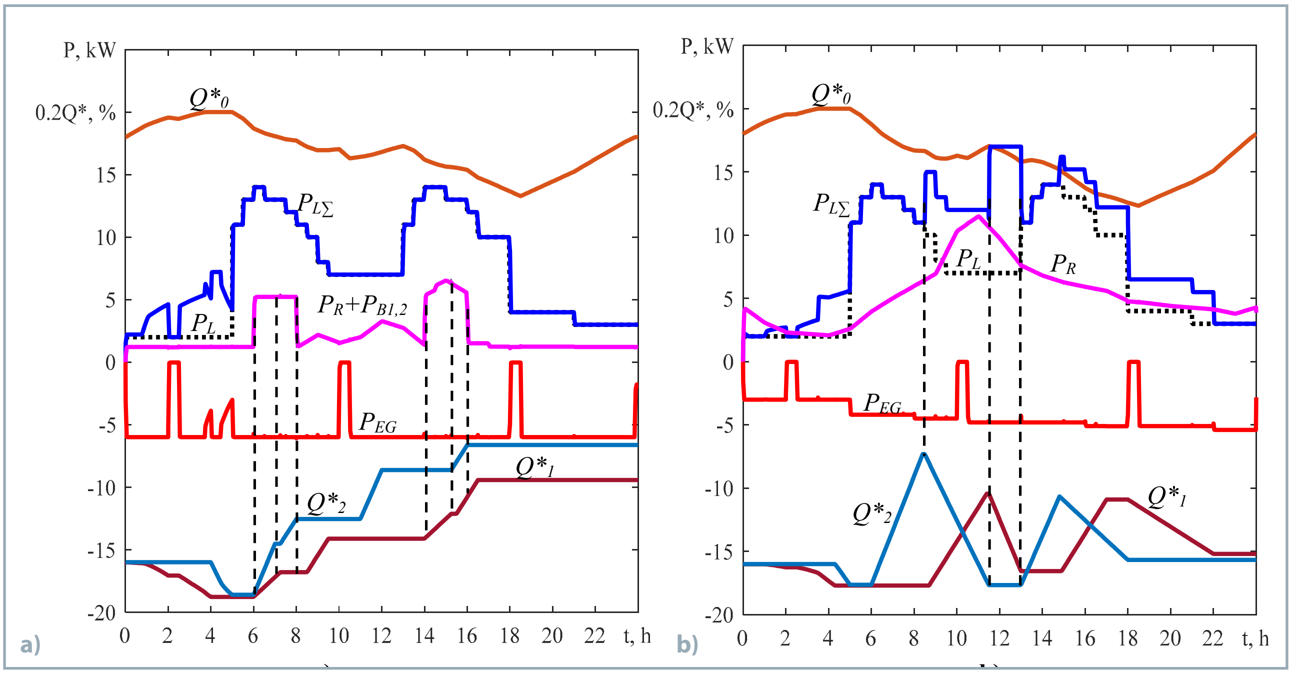

Fig. 3 Process plots for AOM
a) W_R = 36.9 kWh; b) P^*_L = 1 and P^*_R = 1

for two trips of 1 hour with a residual value of Q^*_1 = 47% and Q^*_2 = 33%.

Plots for AOM at P^*_L = 1 and P^*_R = 1 are presented in Fig. 3b. In Fig. 3a, the plots are shown at W_R = 36.9 kWh, when the energy of SB1, 2 ($W_{B12.12}$ + $W_{B12.34}$) = 16 kWh is used for consumption with restriction of the use of ET for 1 hour 2 times a day.

This work is a development of the work by Shavolkin and Haman (2024), where the control of the HRES of a livestock farm was considered with regulation of the value of the power of the battery P_B, which compensates for the deviation of P_R from the P_{RF} forecast and the load P_L relative to the calculated one, while maintaining the value of the power of the EGG P_{EG} within the established limits. The problem of substantiating the parameters of the HRES from the condition of autonomous operation to a day without assessing the effectiveness of the solution for specific generation and load deviations was solved.

A feature of the operation is to ensure an increase in the degree of RES energy consumption with the maximum use of the energy capacity of the main battery and a decrease in energy losses. At the same time, the problem of efficient use of the gas generator, reduction of the main battery's *DoD* and peak consumption during the actual RES generation, taking into account possible changes in the load, is solved. This is achieved by using a closed control system. A schedule of the *SoC* of the main storage battery is controlled. A schedule of power, consumed from the grid with correction by *SoC* deviation, is set.

Restrictions on work results use are related to: a simplified approach using the recommended schedule for the alternate use of ET; during the simulation, the deviation of RES generation and load was realised by a proportional change in the power of RES generation and consumption; the only option to AOM switching at night, which was accepted as the most difficult, was considered.

The solution involves further research on improving the efficiency of using the EGG in emergency AOM in the event of a grid shutdown, and the possibility of using it in normal mode to reduce consumption from the grid with sufficient gas production.

Conclusion

The control mechanism takes into account the SB0 charging characteristic, ensuring that the correction power corresponds to the deviation Q^*, disabling the correction when the PV power is regulated to provide zero export to the grid, and limiting the correction for hours of peak demand. Increasing the use of RES energy and reducing grid consumption (or EGG) is possible due to: adjusting the Q^*_1 value at the beginning of the day according to W_{RF} to increase the degree of use of the SB0 energy capacitance; a daytime charging of the ET batteries during the hours of maximum PV generation with a change in the charging schedule; forming a schedule of $Q^*_R(t)$ with a monotonic decrease in Q^*_R to reduce SB0 energy losses. The alignment of the load schedule also helps reduce energy loss in the SB0.

The exclusion of peak consumption when there is a deviation of RES generation and load can lead to an increase in consumption of up to 2.56%. When limiting peak power to 1 kW, the increase in consumption does not exceed 1.5%. In the case of W_R = 0.85 W_{RF} and the load of 1.15 relative to the calculated one, the value of the *DoD* does not exceed 52%. The reduction of Q^*_2 with full use of RES energy reduces consumption from the grid in load in variant 1 (10.47–16.2)% and in variant 2 (10.8–12.8) %. The monotonous decrease in Q^*_R during the daytime allows for a reduction of losses in the SB0 of about 2 kWh. Changing the charge graph of SB1 and SB2 provides an additional reduction in consumption of about 2 kWh. The overall decrease in consumption in the case under consideration is 4.9%.

References

ABDELSATTAR, M. – ISMEIL, M. A. – ALY, M. M. – ABU-ELWFA, S. S. 2024. Energy management of microgrid with renewable energy sources: A case study in Hurghada, Egypt. In IEEE Access, vol. 12, pp. 19500–19509. DOI: https://doi.org/10.1109/ACCESS.2024.3356556

ALANAZI, M. – ALANAZI, A. – MEMON, Z. A. – AWAN, A. B. – DERICHE, M. 2024. Multi-objective energy management in microgrids: Improved honey badger algorithm with fuzzy decision-making and battery aging considerations. In Energies, vol. 17, no. 17, article no. 4373. DOI: https://doi.org/10.3390/en17174373

AL MUALA, Z. A. – ISSA, M. A. B. – BUGALLO, P. M. B. 2024. Integrating life cycle principles in home energy management systems: Optimal load PV–battery–electric vehicle scheduling. In Batteries, vol. 10, no. 4, article no. 138. DOI: https://doi.org/10.3390/batteries10040138

BOUREK, Y. – MESSINI, E. M. B. – AMMARI, C. – GUENOUNE, M. – CHABIRA, B. – SAHA, B. K. 2025. A hybrid renewable energy system for Hassi Messaoud region of Algeria: Modelling and optimal sizing. In Energy Storage and Saving, vol. 4, issue 1, pp. 56–69.
DOI: https://doi.org/10.1016/j.enss.2024.10.002

DÍAZ-BELLO, D. – VARGAS-SALGADO, C. – ALCÁZAR-ORTEGA, M. – GÓMEZ-NAVARRO, T. 2024. Demand response of prosumers integrating storage system for optimizing grid-connected photovoltaics through time-pricing. In Journal of Energy Storage, vol. 88, article no. 111536.
DOI: https://doi.org/10.1016/j.est.2024.111536

FACCIO, M. – GAMBERI, M. – BORTOLINI, M. – NEDAEI, M. 2018. State-of-art review of the optimization methods to design the configuration of hybrid renewable energy systems (HRESs). In Frontiers in Energy, vol. 12, no. 4, pp. 591–622.
DOI: https://doi.org/10.1007/s11708-018-0567-x

FAKHFOUR, K. – POURFAYAZ, F. 2024. Size optimization of standalone wind-photovoltaics-diesel-battery systems by Harris hawks optimization (HHO): Case study of a wharf located in Bushehr, Iran. In International Journal of Electrical Power & Energy Systems, vol. 163, article no. 110353.
DOI: https://doi.org/10.1016/j.ijepes.2024.110353

GANTHIA, B. P. – PRAVEEN, B. M. – KABAT, S. R. – MOHAPATRA, B. K. – SETHI, R. – BURADI, A. 2024. Energy management in hybrid PV-wind battery storage-based microgrid using droop control technique. In Journal of Mechanics of Continua and Mathematical Sciences, vol. 19, no. 10, pp. 44–66.
DOI: https://doi.org/10.26782/jmcms.2024.10.00004

GUNMI, M. A. – HU, F. – ABU-GHUNMI, D. – ABU-GHUNMI, L. 2024. A smart home energy management system methodology for techno-economic optimal sizing of standalone renewable-storage power systems under uncertainties. In Journal of Energy Storage, vol. 30, article no. 111072. DOI: https://doi.org/10.1016/j.est.2024.111072

IYENGAR, S. – SHARMA, N. – IRWIN, D. – SHENOY, P. – RAMAMRITHAM, K. 2017. A cloud-based black-box solar predictor for smart homes. In ACM Transactions on Cyber-Physical Systems, vol. 1, no. 4, article no. 21, pp. 1–24. DOI: https://doi.org/10.1145/3004056

KHODKAM, H. – POURDARBANI, R. – HERNANDEZ-HERNANDEZ, J. L. 2025. Selection of the most appropriate vehicles with the aim of decarbonising the transportation sector using AHP. In Acta Technologica Agriculturae, vol. 28, no. 2, pp. 63–70.
DOI: https://doi.org/10.2478/ata-2025-0009

KUMAR, K. R. – CHARY, K. P. – NAGARAJU, B. – PRAKASH, K. – KALAVATHI, M. S. 2022. Optimal sizing of grid-connected hybrid solar, wind, and battery energy storage systems. In International Journal of Communication Networks and Information Security (IJCNIS), vol. 14, no. 3, pp. 620–627. Available at:
https://ijcnis.org/index.php/ijcnis/article/view/7711

LAMNATOU, CHR. – CRISTOFARI, C. – CHEMISANA, D. 2024. Photovoltaic/wind hybrid systems: Smart technologies, materials and avoided environmental impacts considering the Spanish electricity mix. In Journal of Sustainable Energy Technologies and Assessments, vol. 70, article no. 103920.
DOI: https://doi.org/10.1016/j.seta.2024.103920

MENG, L. – SANSEVERINO, E. R. – LUNA, A. – DRAGICEVIC, T. – VASQUEZ, J. C. – GUERRERO, J. M. 2016. Microgrid supervisory controllers and energy management systems: A literature review. In Renewable and Sustainable Energy Reviews, vol. 60, pp. 1263–1273.
DOI: https://doi.org/10.1016/j.rser.2016.03.003

OLATOMIWA, L. – MEKHILEF, S. – ISMAIL, M. S. – MOGHAVVEMI, M. 2016. Energy management strategies in hybrid renewable energy systems: A review. In Renewable and Sustainable Energy Reviews, vol. 62, pp. 821–835. DOI: https://doi.org/10.1016/j.rser.2016.05.040

REKIOUA, D. – MOKRANI, Z. – KAKOUCHE, K. – REKIOUA, T. – OUBELAID, A. – LOGERAIS, P. O. – ALI, E. – BAJAJ, M. – BERHANU, M. – GHONEIM, S. S. M. 2023. Optimization and intelligent power management control for an autonomous hybrid wind turbine photovoltaic diesel generator with batteries. In Scientific Reports, vol. 13, article no. 21830. DOI: https://doi.org/10.1038/s41598-023-49067-4

SHAVOLKIN, O. – HAMAN, Y. 2024. Hybrid electric power supply system for a livestock farm using battery electric transport. In Scientific Papers of Donetsk National Technical University, no. 1 (30), pp. 40–51. DOI: https://doi.org/10.31474/2074-2630-2024-1-40-51 (In Ukrainian)

SHAVOLKIN, O. – SHVEDCHYKOVA, I. – KOLCUN, M. – MEDVEĎ, D. 2023a. Improvement of a hybrid solar-wind system for self-consumption of a local object with control of the power consumed from the grid. In Energies, vol. 16, no. 15, article no. 5851.
DOI: https://doi.org/10.3390/en16155851

SHAVOLKIN, O. – SHVEDCHYKOVA, I. – KOLCUN, M. – MEDVEĎ, D. 2022. Improvement of the grid-tied solar-wind system with a storage battery for the self-consumption of a local object. In Energies, vol. 15, no. 14, article no. 5114. DOI: https://doi.org/10.3390/en15145114

SHAVOLKIN, O. – SHVEDCHYKOVA, I. – LISHCHUK, V. – STANOVSKYI, Y. 2023b. Improving a model of the hybrid photovoltaic system with a storage battery for local object's self-consumption involving the setting of power consumed from the grid. In Eastern-European Journal of Enterprise Technologies, vol. 3, no. 8 (123), pp. 6–16.
DOI: https://doi.org/10.15587/1729-4061.2023.280053

THIRUMALAI, S. K. – KARTHICK, A. – DHAL, P. K. – PUNDIR, S. 2024. Photovoltaic-wind-battery and diesel generator-based hybrid energy system for residential buildings in smart city Coimbatore. In Environmental Science and Pollution Research, vol. 31, pp. 14229–14238. DOI: https://doi.org/ 10.1007/s11356-024-32071-0

VACHO, L. – MLINARCSIK, T. – PAULOVIČ, S. 2022. Monitoring of operation of electric system by radiocommunication devices and energy consumption in wastewater treatment plant. In 2022 8th International Conference on Energy Efficiency and Agricultural Engineering (EE&AE). Ruse, Bulgaria, pp. 1–4.
DOI: http://doi.org/10.1109/EEAE53789.2022.9831343

ZEESHAN, S. – AIZED, T. 2023. Design and analysis of a solar energy system for a fruit harvesting robot in Pakistan. In Acta Technologica Agriculturae, vol. 26, no. 4, pp. 185–193.
DOI: https://doi.org/10.2478/ata-2023-0025

ZHANG, C. – ZHANG, M. 2022. Wavelet-based neural network with genetic algorithm optimization for generation prediction of PV plants. In Energy Reports, vol. 8, pp. 10976–10990.
DOI: https://doi.org/10.1016/j.egyr.2022.08.176